Sensing and Imaging (2025) 26:52
https://doi.org/10.1007/s11220-025-00583-9

RESEARCH

Compact CSRR Based Sensor for Detection of Impurities in Liquid Samples

Ameya Vaidya[1] · Kaushik Tvsnd[1] · Antariksh Kalantari[1] · Sandeep Sainkar[1]

Received: 12 February 2025 / Revised: 12 February 2025 / Accepted: 6 April 2025

Abstract

A novel compact RF sensor based on a Complementary Split Ring Resonator (CSRR) for the detection of impurities in liquid samples is designed, developed, and experimentally validated. The sensor uses changes in dielectric permittivity to measure the levels of impurities in common liquids and operates at 2.4 GHz. Two sensor configurations were designed and tested, with different dimensions. The sensor structure's form is intended to achieve increased sensitivity. Because it makes use of the bent form configuration, the sensor structure is fairly compact. The manufactured sensor prototype has a sensitivity of 39.36, which is significantly higher than the sensors found in the literature. A case study was conducted on milk, with water and vegetable oil as impurities and changes in resonant frequency is measured. The sensor provides a 100 kHz shift in the resonant frequency for 50% adulteration. The sensor's compact design, ease of fabrication using a low-cost FR4-Epoxy substrate, and high accuracy make it a viable alternative for non-destructive impurity detection in food safety, healthcare, and environmental monitoring applications.

Keywords Complementary split ring resonator (CSRR) · RF sensor · Dielectric permittivity · Non-destructive testing

1 Introduction

The accurate detection and characterization of impurities in liquid samples is crucial in various industries, including pharmaceuticals, environmental science, and food processing. Traditional methods for detecting these impurities are often costly, time-

✉ Sandeep Sainkar
sandeepsainkar@somaiya.edu

[1] K J Somaiya School of Engineering, Somaiya Vidyavihar University, Mumbai, India

Published online: 29 April 2025

consuming, and may require sophisticated equipment that is not readily available [1]. Recent advancements in sensor technology, specifically RF (Radio Frequency) sensors, have provided an efficient alternative, capable of measuring changes in dielectric properties that indicate the presence of impurities. Various techniques are employed to detect adulteration in milk products. Methods such as infrared spectroscopy and differential scanning calorimetry are discussed in [2]. Conventional chemical tests to identify impurities like sugar, starch, salt, and additionally several approaches for detecting food adulteration are elaborated in [3, 4, 5]. The most common detection method involves the use of chemicals available in labs or test strips. However, a major drawback of test strips is their high cost and the fact that their effectiveness diminishes over time and with exposure to environmental factors [6, 7].

Understanding a material's permittivity is crucial for designing microwave and radio-frequency circuits, antennas, and other electrical systems. It also plays an important role in various industries, such as food quality control, biosensing, and detecting objects underground. The permittivity of a material provides valuable information about its composition, moisture content, and other factors. Since the electrical properties of materials change with these factors, measuring permittivity can help in quality control, monitoring materials, and even detecting changes in biological or environmental conditions [8, 9, 10, 11, 12].

Further advancements in CSRR-based sensors were explored by Buragohain et al. [8], designed a low-cost CSRR sensor for determining the dielectric constant of common solvents. Their sensor, designed to operate at 1.2 GHz and 2.4 GHz, utilized a triple-ring CSRR configuration to enhance field interactions, achieving a sensitivity of 0.87% and accuracy within 4% error. The study highlighted the feasibility of replacing expensive commercial dielectric characterization systems with cost-effective, high-precision microwave sensors. Boybay and Ramahi [9] introduced a CSRR-based sensor etched onto the opposite plane of a microstrip line, forming a band stop filter that enables precise permittivity estimation by analysing frequency shifts in transmission and reflection coefficients. Their work demonstrated high sensitivity in the 0.8–1.3 GHz range, eliminating the need for complex sample preparation. Lee and Yang [10] proposed a planar CSRR sensor for determining dielectric constant and loss tangent of materials using an equivalent RLC circuit. The method enables a single-step, non-destructive measurement process by analysing the resonant frequency shift and magnitude response. Their study demonstrated a CSRR based sensor operating in the 1.8–2.8 GHz range, achieving an error margin below 7.6% in dielectric constant estimation. Extending CSRR applications to food safety, Jain et al. [11] introduced a meander-shaped CSRR sensor for detecting adulteration in edible oils. Their sensor, operating at 801 MHz, exhibited a substantial frequency shift of 275 kHz for 20% adulteration and maintained a high-quality factor of 298. The modified microstrip structure enhanced electric field interaction, improving sensitivity and making the sensor suitable for real-time food quality monitoring. More recently, Chang and Zhang [12] proposed a microstrip antenna sensor incorporating a compressed CSRR on the radiation patch, achieving a significant improvement in sensitivity compared to conventional patch antennas. Their design exhibited a resonant frequency shift from 2 GHz to 1.286 GHz as the dielectric constant varied from 1 to 10, resulting in a 7–7.5 times enhancement in detection performance. These

studies highlight the potential of CSRR-based sensors in dielectric characterization, offering compact, low-cost, and highly sensitive solutions for industrial and scientific applications.

In this work, two novel complimentary split spring resonator (CSRR) structures with different substrate dimensions have been proposed. The later design incorporates a modified microstrip line to provide a compact, highly sensitive sensor that can detect impurities in liquids. The results were validated by comparing them with simulations of the sensor conducted using ANSYS HFSS. The sensor requires only a minimal amount of sample, and is designed to test a broad range of liquid samples. Furthermore, the proposed sensor can be used to resolve the potential problem as depicted in [14].

The paper is organized in four sections. Section II discusses the design and development of the sensor; Section III covers the result and the discussions and section IV includes the conclusions.

2 Sensor Design and Development

A Closed Loop resonator-based patch antenna sensor, after a series of design steps, variations, and parametric analysis, was made with Square Loop and two open end stubs, resembling an equal to sign (=) [6]. This design was further converted to a CSRR configuration, replacing the SRR configuration to achieve better field concentration and sensitivity. A ring was further added by extending the outer arms of the SRR structure to improve the Electric Field concentration between them. To provide excitation to the CSRR, an electric field perpendicular to the CSRR is required. This was achieved by using a microstrip transmission line with the CSRR etched onto the ground plane. The resulting structure resembles a typical stopband filter. When a sample is placed on the CSRR, the resonant frequency of the CSRR shifts, leading to a change in the filtering characteristics. All the dimensions (in mm) have been tabulated in Table 1.

A novel complimentary split spring resonator (CSRR) structure with different substrate dimensions has been designed to operate at 2.4 GHz with a modified microstrip line, of 120 mm x 40 mm and 50 mm x 25 mm respectively. The sensor was designed with a microstrip line of 3 mm width for the 120 mm configuration, whereas the 50 mm configuration was designed with a bent configuration of a microstrip line as shown in Fig. 1. (b) [13], having 3 mm width, to reduce the length of the sensor and make it compact. In both of these configurations, the same CSRR was used as shown in Fig. 1. (a). In the 120 mm configuration, the split ring gap is 4 mm, whereas in the 50 mm configuration, the split ring gap is 0.9 mm. To keep the cost low, these sensors have been designed using commercially available and cheap FR4-Epoxy substrate,

Table 1 Dimensions (in mm)

Cx	Cy	Ix	Iy	Go	Gi	Sx	Sy	Sh
9.58	8.77	7.43	6.25	1	0.7	3	0.5	2.3
L1	**L2**	**L3**	**L4**	**W**				
16	13	4	24	3				

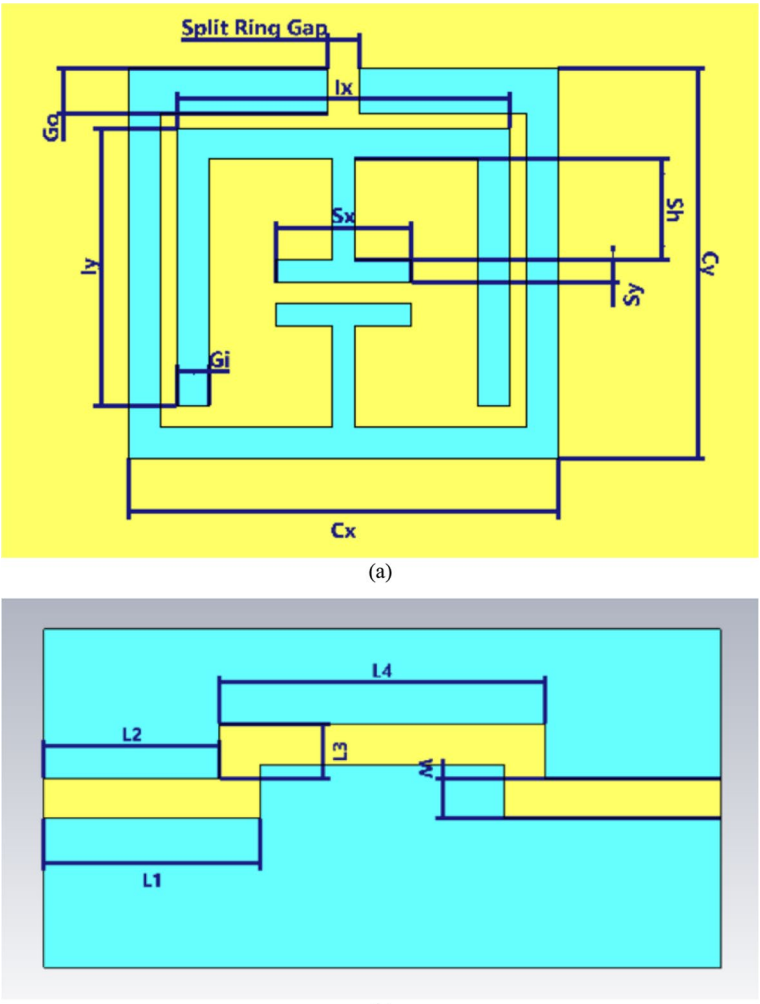

Fig. 1 Schematic Diagram (**a**) Top View (**b**) Bottom View

with dielectric constant 4.4, which has a thickness of 1.6 mm. The thickness of the copper layer is 0.035 mm. All the design and simulations have been carried out using Ansys HFSS. After fabricating the sensors according to the designs shown above, SMA connectors are connected on both sides of the sensor, as can be seen in Fig. 2. Resonant frequency can be accurately tuned, if required, by applying a copper tape over the split ring gap, which alters the size of the gap without affecting the fabricated structure.

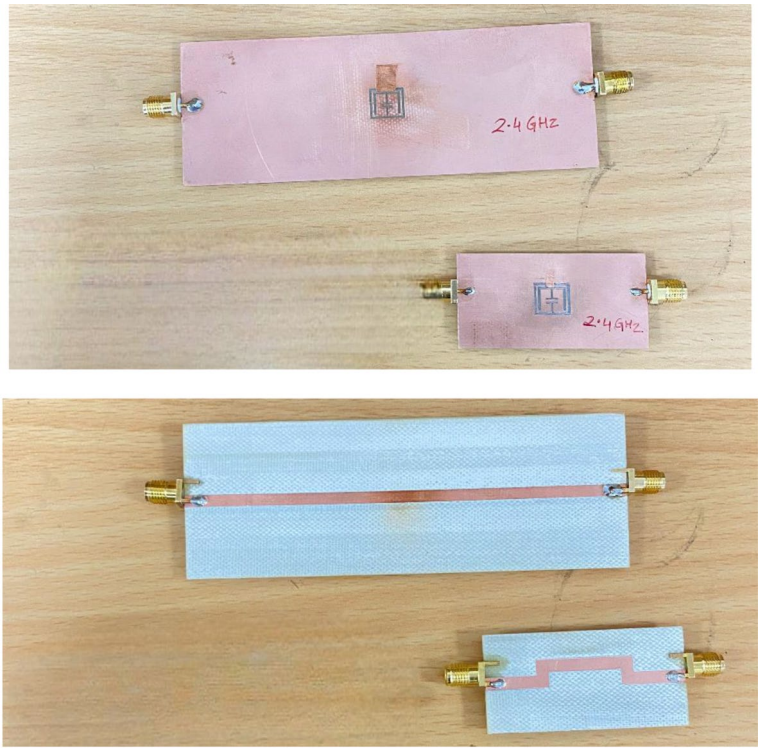

Fig. 2 Fabricated CSRR Sensor configurations

3 Results and Analysis

In this section, the proposed sensor is analysed initially, by using simulation software and later, using actual samples tested with the fabricated sensor. In the software analysis, a domelike shape is kept on top of the CSRR. We can change the dielectric constant of this material so that it resembles the LUTs. The observations on analysing the electric field, scattering parameters, volume of the domelike shape placed on top of the CSRR and the calculation of sensitivity is discussed further.

3.1 Simulated and Measured Results of the Sensor

Simulated *S*-parameters for both configurations are shown in Fig. 3. The electric field distribution around the CSRR Structure is shown in Fig. 4. It is observed that maximum field is concentrated near the bottom of the sensor, which is where the LUT will be placed in the sensing region because it facilitates increased electric field interaction with LUT to improve the sensitivity.

A slight change in the *S*-parameters is observed from the simulated values due to limitations and errors during fabrication, and also due to external sources present around the sensor, as opposed to vacuum, which we had used for simulation purpose, as shown in Fig. 5.

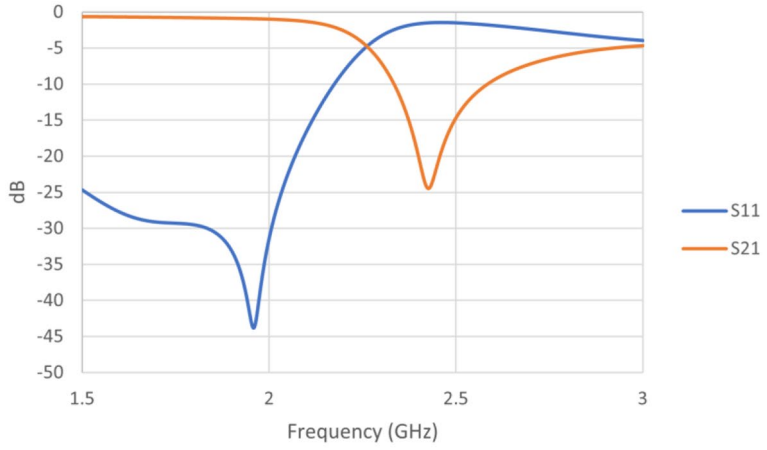

(a)

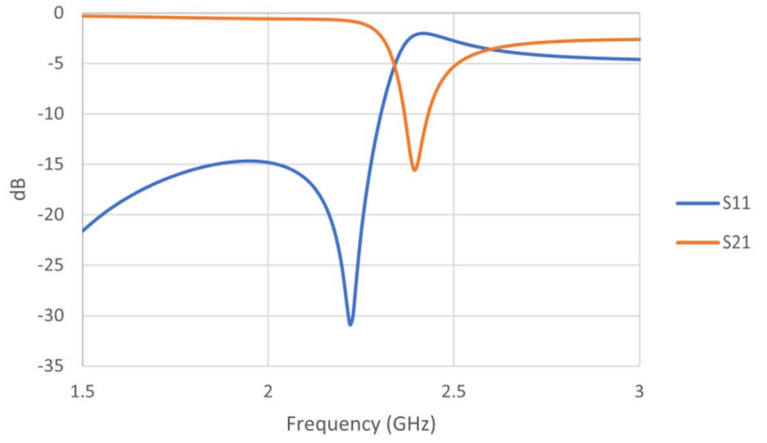

(b)

Fig. 3 Simulated S-Parameters of (**a**) 120 mm configuration (**b**) 50 mm configuration

3.2 Sensor Analysis

A CSRR can work like a sensor based on the interaction between the samples (with certain dielectric permittivity) loaded and electromagnetic waves. The microstrip line at the back side of the sensor is capacitively coupled with the CSRR placed at the front. The sensing phenomenon is because of the change in dielectric permittivity at the region having maximum field concentration where the material is loaded on to the sensor based on the relation of Capacitance with Area, Permittivity and distance between the parallel plates of the Capacitor (Eq. 1).

$$C = \frac{\in_0 \in_r A}{D} \tag{1}$$

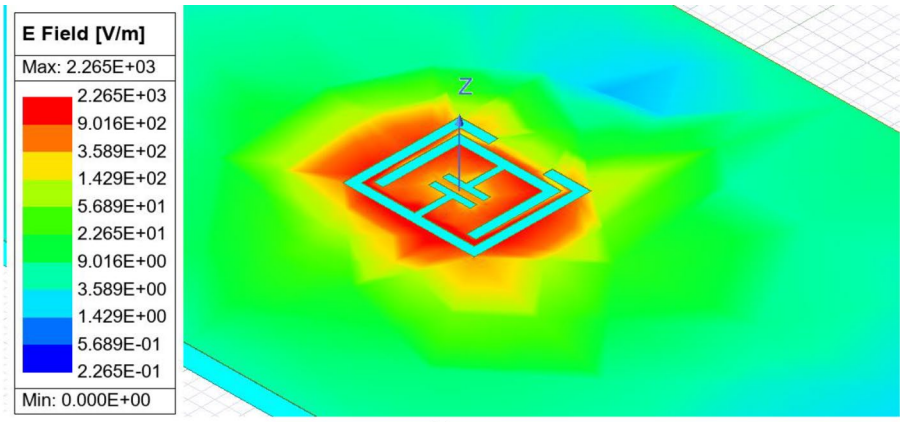

(a)

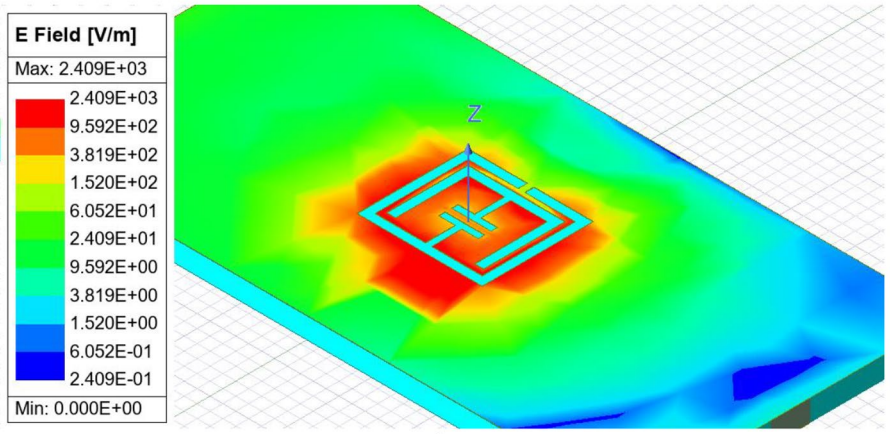

(b)

Fig. 4 Electric Field Distribution (**a**) 120 mm configuration (**b**) 50 mm configuration

where C is the capacitance, $\in_0$ is the permittivity of vacuum, $\in_r$ is the relative permittivity, and A is the area of the region having maximum field concentration. When different materials are made to contact with the CSRR, the fringing field effect changes, hence, the permittivity of the material has influence on all the sensor properties. The performance of the sensor was then computed using Eq. 2 [8] and compared with the sensors available in the literature.

$$S = \frac{\Delta F}{\Delta \in} \tag{2}$$

$$Where\ \Delta F = |F_0 - F, LUT|\ and\ \Delta \in = |1 - \in, LUT|$$

We normalize the sensitivity before comparing the sensors because the operating frequencies of the sensors proposed by other authors vary and the sensors running at higher frequencies exhibit greater shifts in resonant frequency when a sample is

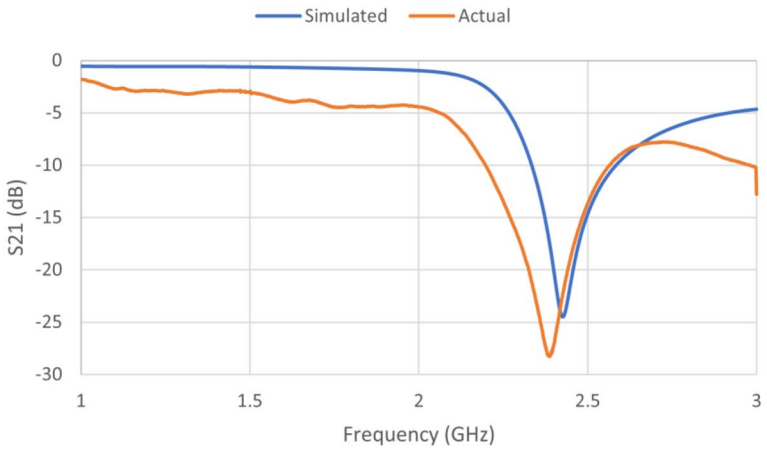

(a)

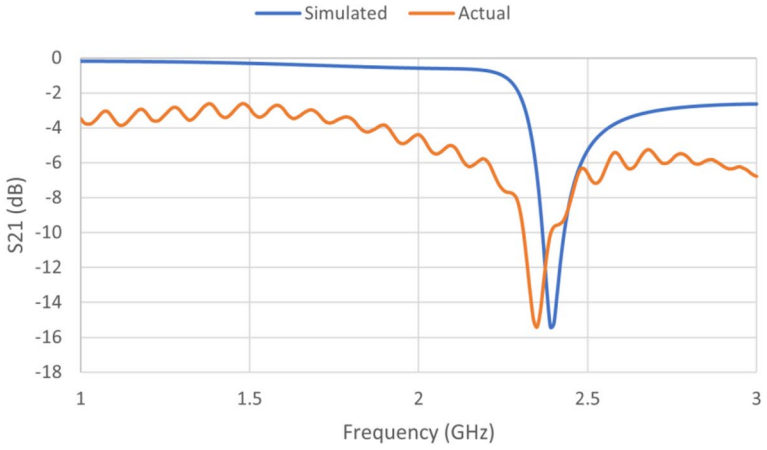

(b)

Fig. 5 Simulated and measured S_{21} for (**a**) 120 mm configuration (**b**) 50 mm configuration

placed on top of them. For this reason, the authors have calculated the $Savg, f\,(\%)$ in percentage terms by dividing the sensitivity S by the sensor's resonance frequency (F_0), as expressed in Eq. 3.

$$Savg, f\,(\%) = \frac{S}{F_0}100\% \tag{3}$$

Figure 6 shows the setup of the sensor loaded with the sample placed at the region having maximum field concentration. A hemispherical structure modelled in HFSS is used to resemble various common solvents and liquids such as Acetic Acid, Acetone, Methanol, Distilled Water, etc.

The resonant frequency of the sensor is found to decrease as the relative permittivity of the LUT increases when the relative permittivity of the hemispherical structure

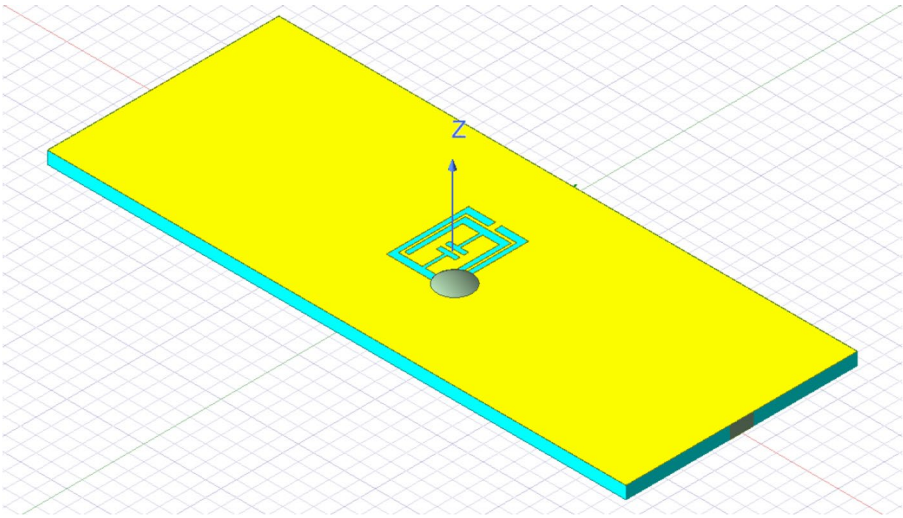

Fig. 6 Sensor loaded with LUT

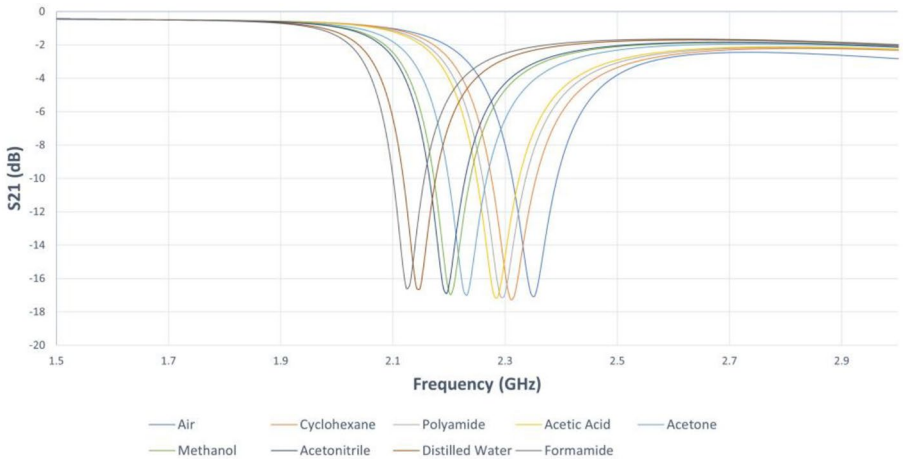

Fig. 7 Variation of Resonant Frequency of the Sensor

simulated in HFSS, as depicted in Fig. 6, is varied. Figure 7 shows a visualization of this. As seen in Fig. 8, the shift in the resonant frequency plots for several samples is noted.

Hence, a sensitivity of 39.36 and relative sensitivity $S_{avg,\ f(\%)}$ of 1.64% was obtained, which is significantly higher than other proposed works. The comparison of the sensor designed in this work with existing works in the literature is presented in Table 2.

The sensitivity of the 50 mm structure is higher than the 120 mm structure and other proposed works. This is due to the Electric field concentration at the sensing

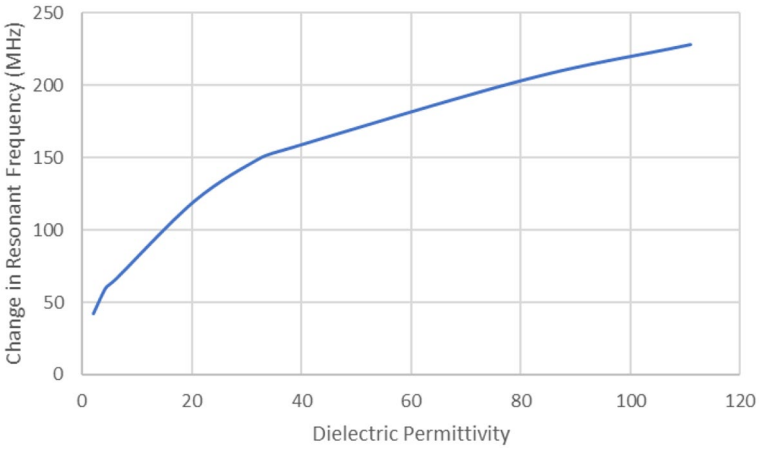

Fig. 8 Shift in Resonant Frequency for different liquids

Table 2 Comparison with existing works

Reference	Fo (GHz)	S	Savg, f(%)	Permittivity Range	Overall Size(mm^2)
[6]	2.48	13.7	0.55	1-100	1505
[8]	2.335	20.525	0.879	1-80.1	3000–4800
[11]	7.84	10.2	0.13	2–3	Not specified
[12]	2.6	0.27	0.375	2–10	6400
This work	**2.4**	**39.36 8.82**	**1.64 0.36**	**1–81 1–81**	**4800 (120 mm configuration) 1250 (50 mm configuration)**

region being higher in the 50 mm structure as compared to the 120 mm structure as sensitivity is directly linked to Electric field concentration.

3.3 Experimental Results of the Sensor with Water and Vegetable Oil

In this section, the fabricated Compact CSRR based sensor, has been experimentally tested. A case study is presented for the detection of impurities in milk, perturbed with water and vegetable oil. The testing of milk with water and oil as impurities is shown experimentally. Different quantities of water are added to milk as impurity and the change in resonant frequency and S21 are noted. The authors have tested for three different cases, starting with 100% Milk, followed by 50% Milk and Water each, then 75% water and 25% milk. The same quantities of Vegetable Oil are added to milk and the same process is repeated. The authors have selected Water and Vegetable Oil as impurities as they are two of the most common and readily available adulterants of milk, used to increase the volume and fat content of milk respectively. Since the samples cannot be put in direct contact with the sensor, they have been placed in the cap of a commercially available bottle. The volume of sample in the cap has been kept 2.5 ml throughout this testing, and it is kept on top of the CSRR, which has

maximum Electric field concentration, as shown in Fig. 6. The test setup is shown in Fig. 9 and the variation of resonant frequency on adding quantities of impurities to milk is shown in Fig. 10. The sensor provides a 100 kHz shift in the resonant frequency for 50% adulteration of water in milk.

The concentration and material characteristics of the impurity in the sample placed onto the sensor determine how the operating frequency and S_{21} are changed when test samples are added. It is possible to calculate the amount of water and oil that are added to milk as adulterants based on the analysis results. Variations in frequency and S_{21} are caused by variations in the sample's relative permittivity.

3.4 Experimental Results of the Sensor by Varying Volume of the LUT

An additional case study is presented, by varying volumes of Water, Vegetable Oil and Acetone respectively from 0.5 ml to 2 ml. The testing of water, oil and acetone is shown experimentally. The authors have used the 120 mm configuration for this case study. The variation of resonant frequency on adding quantities of liquids is shown in Fig. 11.

This seeks to replace the Ultrasonic Sensor, which was used in [17] to determine the volume of fluid in the bottle and, consequently, the drip rate. The authors had placed the sensor into the very end of the IV fluid bottle. The inability to insert the Ultrasonic Sensor into the IV fluid bottle while the patient is receiving it is a possible issue with this method. Using an RF sensor instead of an ultrasonic sensor, which likewise experiences frequency fluctuation when the volume of LUT is changed, is therefore one possible option, as previously shown. The exact volume of liquid present in the bottle cannot yet be detected by the RF sensor, but a method for doing so could be developed in the future, which would also remove the requirement for the large and costly Vector Network Analyzer.

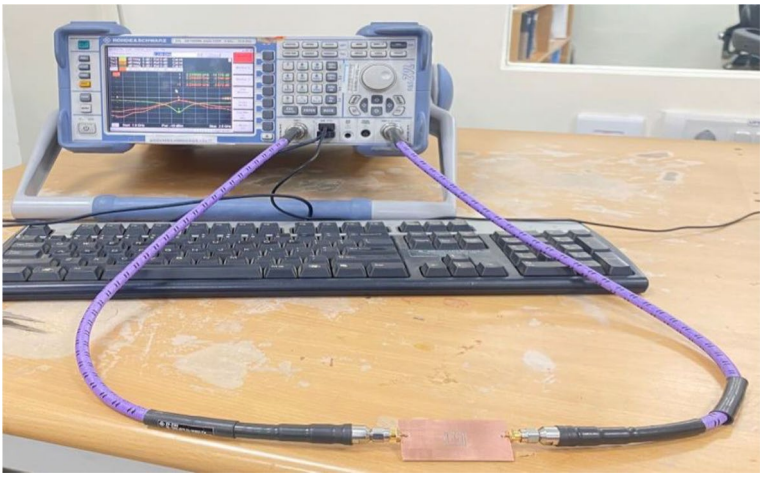

Fig. 9 Measurement Test setup

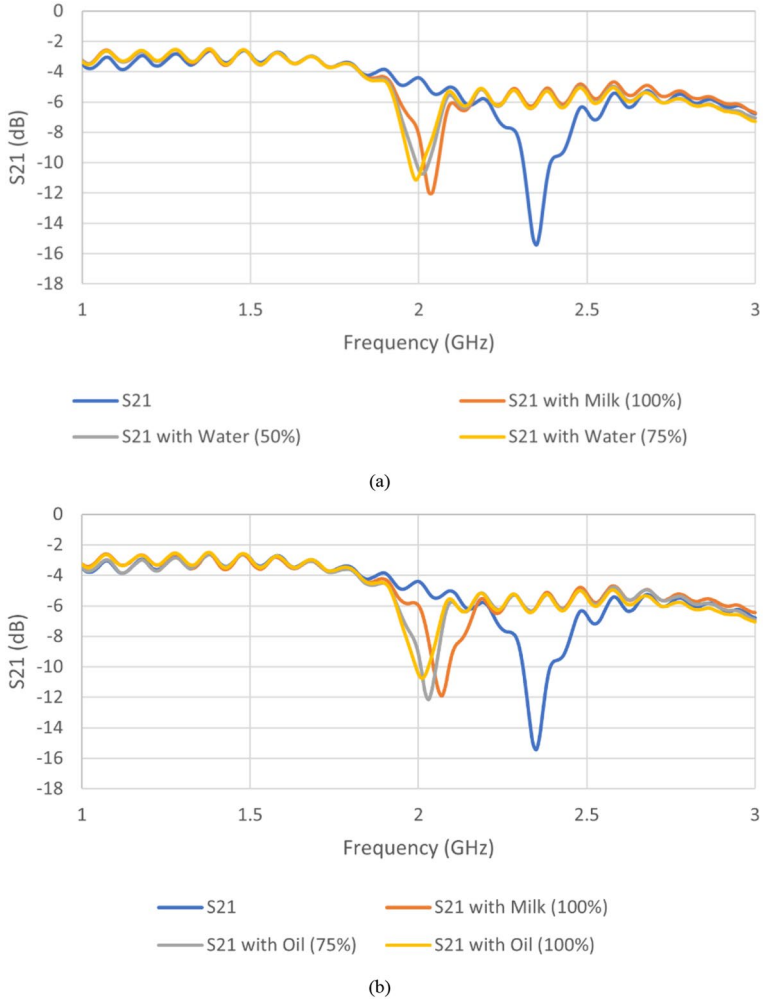

Fig. 10 Variation of Resonant Frequency with (**a**) Water (**b**) Vegetable Oil

4 Conclusion

In this work, the design of a planar CSRR-based Microstrip Sensor has been discussed for the purpose of impurity detection based on a non-destructive testing approach. The sensitivity of the sensor has been determined, first by using simulation software, and then, experimentally. The adulteration in Milk, by using Water and Vegetable Oil as impurities has been studied by observing the variation in frequency, depending on the permittivity of the impurity added. This determines the percentage of impurity added. It has been observed that the relative permittivity of the impurity added has an inverse relationship with the resonant frequency of the sensor. Results show that the sensor designed in this work has sensitivity of 39.36, able to differentiate materials with varying dielectric constants. Testing across a broad range of dielectric constant

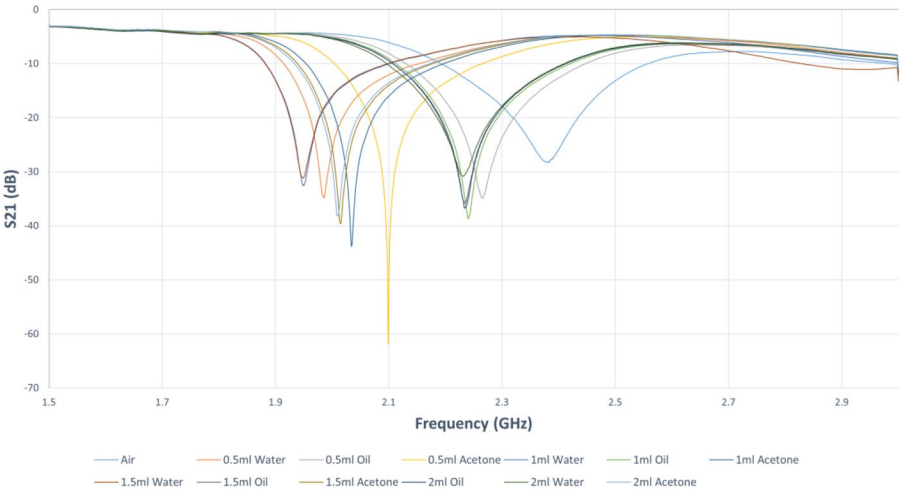

Fig. 11 Variation of Resonant Frequency with varying volumes of LUT

values confirms the sensor's effectiveness, highlighting its potential for both industrial and commercial applications. Another benefit of this structure is that it is simple to incorporate into microwave circuits.

Acknowledgements The authors wish to acknowledge the Electronics and Telecommunication Engineering department, K.J. Somaiya School of Engineering for their constant support and guidance. The authors are also grateful to Birla Institute of Technological Sciences, Hyderabad Campus for letting them use their facilities for the successful completion of this work.

Author Contributions A.V. and K.T. wrote the main manuscript text and A.V. prepared figures and tables. S.S reviewed the manuscript.

Data Availability No datasets were generated or analysed during the current study.

Declarations

Competing Interests The authors declare no competing interests.

References

1. Kamthania, M., Saxena, J., Saxena, K., & Sharma, D. K. (2014). Milk adultration: Methods of detection & remedial measures. *International Journal of Engineering and Technical Research*, *1*, 15–20.
2. Poonia, A., Jha, A., Sharma, R., Singh, H. B., Rai, A. K., & Sharma, N. (2017). Detection of adulteration in milk: A review. *International Journal of Dairy Technology*, *70*(1), 23–42.
3. Azad, T., & Ahmed, S. (2016). Common milk adulteration and their detection techniques. *Int J Food Contamination*, *3*(1), 1–9.
4. Prasanth, P., Viswan, G., & Bennaceur, K. (2021). Development of a low-cost portable spectrophotometer for milk quality analysis. *Mater Today Proc*, *46*, 4863–4868.
5. Krishnan, R. G., & Saraswathyamma, B. (2021). Disposable electrochemical sensor for coumarin induced milk toxicity in Raw milk samples. *Measurement*, *170*, Art108709.

6. Aishwarya, S., Meenu, L., Menon, K. U., Donelli, M., & Menon, S. K. (2023). A novel microstrip sensor based on closed loop antenna for adulteration detection of liquid samples. *IEEE Sensors Journal*.
7. Tiwari, N. K., Singh, S. P., & Akhtar, M. J. (2018). Novel improved sensitivity planar microwave probe for adulteration detection in edible oils. *IEEE Microwave and Wireless Components Letters*, *29*(2), 164–166.
8. Buragohain, A., Mostako, A. T. T., & Das, G. S. (2021). Low-cost CSRR based sensor for determination of dielectric constant of liquid samples. *IEEE Sensors Journal*, *21*(24), 27450–27457.
9. Boybay, M. S., & Ramahi, O. M. (2012). Material characterization using complementary split-ring resonators. *IEEE Transactions on Instrumentation and Measurement*, *61*(11), 3039–3046.
10. Lee, C. S., & Yang, C. L. (2014). Complementary split-ring resonators for measuring dielectric constants and loss tangents. *IEEE Microwave and Wireless Components Letters*, *24*(8), 563–565.
11. Jain, S., Azad, P., Tiwari, N. K., & Akhtar, M. J. (2023). Design of Complementary Meander Shaped Resonator for Adulteration Testing, *IEEE Microwaves, Antennas, and Propagation* Conference *(MAPCON)* (pp. 1–4).
12. Chang, S., & Zhang, W. (2022). Microstrip Antenna Sensor for Dielectric Constant Detection of Solid-state Media, International Applied Computational Electromagnetics Society Symposium (ACES-China) (pp. 1–3). IEEE.
13. Al-Gburi, A. J. A., Zakaria, Z., Abd Rahman, N., Alam, S., & Said, M. A. M. (2023). p.384, A compact and low-profile curve-feed complementary split-ring resonator microwave sensor for solid material detection. *Micromachines*, 14(2).
14. Srivatsan, R. N., Rolia, N. A., Bharj, G. S., Sainkar, S., Gupta, S., & Kelkar, K. (2024). Design and Development of Drip Monitoring of IV System, International conference on *Technologies for Energy, Agriculture, and Healthcare* (pp. 424–432).